Astron. Astrophys. 354, 943–959 (2000)

ASTRONOMY AND ASTROPHYSICS

Mixing by internal waves

III. Li and Be abundance dependence on spectral type, age and rotation

J. Montalbán[1] **and E. Schatzman**[2]

[1] Instituto de Astrofísica de Canarias, 38200 La Laguna, Tenerife, Spain
[2] DASGAL, URA CNRS 335 Observatoire de Paris-Meudon, 92195 Meudon, France

Received 19 April 1999 / Accepted 29 November 1999

Abstract. In this paper we deal with the problem of the generation of internal waves at the bottom of convective zone in solar-type stars, and with the transport process linked to the non-adiabatic propagation of these waves through the stable radiative region. The main improvement with respect to the previous papers in this series comes from the convection treatment chosen in order to describe the perturbations exciting the internal waves at the boundary convective/stratified zones. We consider a model of convective transport by plumes as described by Rieutord & Zahn (1995), taking into account the presence of overshooting as modelled by Zahn (1991). A model of convective transport by plumes implies that it is no longer necessary to introduce an *ad hoc* parameter to emulate the consequences of asymmetric downward and upward flows, as was the case when a classical description of the convection was adopted.

The velocity field produced in the stellar interior by gravity waves provides a diffusion coefficient. The predictions of this transport process for light element abundances in low-mass stars reproduce the observational features of lithium abundance: its dependence on mass and age. Furthermore, a phenomenological treatment of the interaction rotation/overshooting based on numerical simulations of the penetrative convection with and without rotation (Julien et al. 1996a, 1997a) provides a more or less efficient mixing process depending on the rotational state of the star and reproduces the observed "correlation" between lithium abundance and rotational velocity and the scatter of lithium abundance in stars of the same age, mass and chemical composition.

The dependence of the diffusion coefficient on the depth below the convective zone is tested by comparing the prediction for Be abundance with the available observations. The results are also in good agreement, but the uncertainties in the observations are too large.

Key words: convection – stars: evolution – stars: interiors

1. Introduction

The light elements, lithium and beryllium are fragile atoms susceptible of being destroyed at low temperatures by fusion reactions. The degree to which Li and Be are depleted from stellar atmospheres serves as a tracer of internal stellar kinematics. These elements provide useful information about the regions beneath the convective zone in cool stars in tracing the redistribution of material and mixing patterns inside the star. Spectroscopic studies of Li and Be therefore expose otherwise hidden stellar interiors and set up a guide in the search for physical processes that should be incorporated in the treatment of the structure and evolution of stars.

During the last thirty years a great deal of work has been devoted to the measurement of atmospheric lithium abundance in a comprehensive set of stars. Observations in open clusters of different ages and in field stars (e.g. Duncan 1981; Duncan & Jones 1983; Cayrel et al. 1984; Balachandran et al. 1988; Boesgaard et al. 1988; Soderblom et al. 1990; Thorburn et al. 1993; Soderblom et al. 1993a,b,c; Pasquini et al. 1994; García López et al. 1994; Balachandran 1995; Soderblom et al. 1995; Jeffries 1997) show that the mean features of lithium abundance among Pop I stars (here we deal with late F-, G- and K-type stars) are: *i)* at a given metallicity, the Li surface abundance in late-type stars is a decreasing function of both effective temperature, or mass, and stellar age. *ii)* there exists a spread in Li among late-type stars of the same colour, in young clusters and in field stars. Furthermore, the lithium abundances observed in T Tauri stars (Martín et al. 1994, and references therein) and in clusters with different ages (e.g. α Per by Balachandran et al. 1988; the Pleiades by García López et al. 1994; the Hyades by Cayrel et al. 1984; and M 67 by Balachandran 1995) show that for low-mass stars part of the lithium is destroyed during the PMS phase, and that the atmospheric lithium depletion goes on during the main sequence stellar lifetime.

This behaviour cannot be explained in the framework of the standard model of internal structure and stellar evolution, and indicates that some physical processes have been forgotten in the stellar modelling. Transport processes may remove these delicate nuclei from the convection zone to depths where temperature is high enough to destroy them, producing, in this way, a redistribution of matter in the star. In parallel with observational discoveries, different mechanisms have been proposed to explain these observational data (see Michaud & Charbonneau 1991 for a review). Thus, observations of lithium abundances and stellar rotation inside young clusters such as the Pleiades

Send offprint requests to: J. Montalbán

and α Per (Balachandran et al. 1988) showed that in young clusters there is a "correlation" between lithium abundance and stellar rotation (i.e. for the same mass the higher the rotational velocity the higher the lithium abundance). This fact led to the development and acceptance of models that link chemical mixing to angular momentum loss (AML), the evolution of lithium abundance and its spread being a consequence of angular momentum history (Pinsonneault et al. 1989, 1990; Chaboyer & Zahn 1992; Zahn 1992). The most serious objection against these models comes from the discrepancy between the internal rotational gradient predicted for the Sun and helioseismological measurements. The mechanism described by Zahn (1992) does predict that young, fast rotators should have higher lithium abundances, as is observed. This theory also predicts that the Sun should have a rapidly rotating core; however, Eff-Darwich & Korzennick (1998) find that the Sun's interior rotates as a solid body down to $r/R_\odot \sim 0.2$. Furthermore, recent models by Chaboyer et al. (1995) are able to account for the observed lithium depletion, but only at the expense of having a large solar inner angular velocity.

Schatzman (1991), using the results presented by Press (1981), proposed an alternative transport process in which the chemical mixing is induced by the non-adiabatic propagation, in the stellar radiative interior, of the internal waves generated at the boundary of the convective zone. Several papers have been devoted to this transport process and have provided certain improvements in the mathematical and physical treatment of the generation of internal waves, and in the treatment of diffusive process in stellar radiative interiors (Montalbán 1994; Schatzman & Montalbán 1995; Schatzman 1996). Montalbán (1994, Paper I) and Montalbán & Schatzman (1996, Paper II) applied the diffusion coefficient to estimate its role in lithium and beryllium depletion in the Sun and in Pop I stars with masses between 0.7 and 1.2 $\mathrm{M}_\odot$ of the age of the Hyades (8.10^8 yr). The comparisons with observational data were quite satisfactory. However, the need for a phenomenological adjustment of a basic parameter in order to cancel the known underestimation of the convective velocity by mixing length theory (MLT), raised doubts about the model. In this paper we have treated the generation of internal waves within the framework of the model of convective transport by plumes developed by Rieutord & Zahn (1995). Therefore, we do not need to introduce an *ad hoc* parameter to adjust the vertical velocity of turbulent motions. In Sect. 2 we present the physical description of the models as well as the improvements with respect to previous treatments. In Sect. 3 we give the expression of the new diffusion coefficient and we analyse its dependence on turbulence features. In Sect. 4 we apply this diffusion coefficient in order to estimate the lithium abundance in stars with solar metallicity, in a mass range from 0.7 to 1.2 $\mathrm{M}_\odot$. We compare these theoretical results with observational data in clusters with ages from 10^8 yr to solar age.

Concerning the above-mentioned spread of lithium, it is nowadays widely accepted that lithium abundance is not only a function of mass, age and chemical composition, but that there is a fourth factor affecting the evolution of lithium abundances in late-type stars, and that this factor should be stellar rotation. However there is no agreement concerning *how* the stellar rotation works. This disagreement is specially due to our poor knowledge of the physical process associated with rotation, and of the interaction between rotation and other physical processes inside the stars. The effects of stellar rotation on stellar structure and the location of the base of the convective zone during the PMS phase have been analysed by Martín & Claret (1996). During the PMS phase of low-mass stars a small variation in structure can produce observable differences in lithium abundance. Numerical simulations of rotating convection by Julien et al. (1996a,b, 1997a,b) and Brummell et al. (1996) show that the rotation modifies the characteristics of the flow in the convective region. In particular Julien et al. (1996a, 1997a) study the effect of rotation on the overshooting depth and on the plume features in the penetration region. There is no doubt that stellar rotation is a complex and poorly-known phenomenon, and that, therefore, in addition to the angular momentum transport in the interior and its effects, there could be other processes to be considered in the study of the consequences of rotation on stellar structure and evolution. We cannot reject interactions between rotation and convection, or the effects of rotation on the generation of internal waves and their propagation. In the present state of the art, it is not possible to rule out any of these. In Sects. 4.2 and 4.3 we use a phenomenological and simple treatment (based on of the results of Julien et al. 1996a, 1997a) of the influence of rotation on the characteristics of overshooting. We show that, when a possible effect of stellar rotation on internal wave generation and propagation is taken into account, the spread of lithium abundance and its connection to stellar rotation can also be explained within the framework of the internal wave diffusive process.

Another important test that any mixing mechanism must pass is the Be abundance test. In fact, beryllium is burned at higher temperatures the lithium; consequently, a transport process with the appropriate dependence on depth below the convective zone must be able to reproduce the Be abundance observed and its dependences. In Sect. 4.4 we present the Be abundances predicted by our mixing mechanism and the comparison with the available observational data.

2. Physical description of the model

2.1. Some physical aspects of the problem

The structure of solar-type stars ($\mathrm{M} < 1.3\ \mathrm{M}_\odot$) presents an envelope where the heat transport is effected essentially by convective motions. Because of the low viscosity of stellar plasma, this convective flow is strongly turbulent. Beyond the surface of the convective zone, we find a region where the matter remains in stable stratification, and the heat transport is effected by radiation. The standard solar model (SSM) assumes that both regions are separated by a rigid surface, and that there is no interaction between the turbulent and the stable domains. The position of this surface is given by the Schwarzschild criterion of stability, which means that the convective motion stops when the gradient of temperature in the star is equal to the adiabatic gradient,

that is, when the buoyancy force disappears and the acceleration becomes zero.

However, the boundary between the turbulent envelope and radiative interior is neither rigid nor impermeable. The turbulent fluid elements do not stop immediately in the stable region, but penetrate a small distance before their vertical velocity becomes zero (e.g. Zahn 1991 and references therein). These incursions of turbulent elements in the stable region can, if the efficiency of the convection is large enough, influence the sub-adiabatic stratification and impose an adiabatic or quasi-adiabatic regime beyond the boundary determined by the Schwardchild criterion (penetrative convection). If the convection is weak enough, there will be a spread of mixed layer, but no change in the structure of this extended mixed layer (overshooting).

That phenomenon of overshooting (in a wide sense) has important consequences for our problem of light-element burning: firstly, it involves an extra spreading of the mixed region, and secondly, the perturbation produced in the region with stable stratification generates internal waves that can propagate beyond the limit of the convective layer, inside the radiative interior.

To describe the diffusive processes linked to the non-adiabatic propagation of these waves as suggested above, it is necessary to know the velocity field in the radiative interior and to solve the corresponding equation of motion.

The equation of motion in the radiative zone is (in the adiabatic case) a non-homogeneous wave equation:

$$\frac{d^2\Psi}{dr^2} + \left(\frac{N^2}{\omega^2} - 1\right) k_{\rm H}^2 \Psi = S(\mathbf{r}, t). \quad (1)$$

The non-homogeneous term $S(\mathbf{r}, t)$ (the source function) consists mainly of terms of the Reynolds tensor, which represents the momentum flow produced by the fluctuating velocity field. It can be interpreted as an external force working on the radiative interior through the elements of a turbulent fluid which arrive at the boundary of the convective zone.

The solution of the mathematical problem involves a knowledge of the boundary conditions, therefore the determination of the wave amplitude in the radiative interior depends on the description of the velocity field on the other side of the boundary. In order to consider the effect of overshooting on atmospheric abundances, we not only need to know the depth of the extra-mixed region, but also to have a good characterization of turbulent motions in the convective penetration region. Both of these are inaccessible at present since a knowledge of them would require the solution of the dynamical equation for a convective and turbulent system. Taking into account the present state of the art, the only approach to the problem is to use the phenomenological description provided by various attempts to reproduce as closely as possible the real properties of turbulent convective flow.

2.2. Concerning convection

Stellar convection is compressible convection with completely developed turbulence over several pressure scale heights. Unfortunately, in these conditions, the theoretical treatment of convective motions and convective transport is not simple.

In astrophysics the stellar convective zone is usually modelled using the mixing length theory (MLT), where the heat transport occurs through the exchange of macroscopic fluid elements. These fluid elements (with a size of the order of one pressure scale height) travel with velocity v over a distance L (of the order of the mixing length), after this the element is dissolved in the medium. This theory is based on the Boussinesq approximation, and uses convective theories developed to deal with convection in laboratory and geophysical fluids. It provides local computation of convection at every point of the convective region. Despite all these limitations, this theory allows the global properties of stars to be reproduced. However, it does not say anything about the structure of the convective zone, or about the boundary conditions. Thus, there are manifestations of a completely developed turbulence, such as convective penetration and overshooting, which cannot be described by MLT.

There has been a great number of approaches to the modelling of the non-local aspects of convection (for reviews see Spruit et al. 1990; Massaguer 1990). Although none of these treatments is able to set up a procedure to be introduced easily in the computation of stellar models; nevertheless, they provide very useful information on the phenomenology of convective motions. In particular, numerical simulations of turbulent convection in a stratified medium (Cattaneo et al. 1991; Stein & Nordlund 1989) have revealed that the convection is highly compressible and intermittent, with very strong downward flows forming structures of long temporal duration, and very slow outward motions without well defined structure.

These turbulent structures (plumes) have also been observed (Turner 1986 for a review) in laboratory experiments, and in the Earth's atmosphere above very concentrated sources of heat. It seems that plumes could also be very important in the dynamics of stellar convective zones. Rieutord & Zahn (1995, hereafter RZ95) proposed a model of compressible stellar convection in which the energy is transported by plumes generated in the upper boundary of the convective zone, in which the super-adiabatic gradient is very steep, by strong temperature and density fluctuations. These currents of turbulent fluid flow through the convective zone, from the level where they are produced to the bottom of the convective zone. As they travel the currents drag matter from the surrounding medium because of the instabilities in their lateral boundary. The quantity of matter dragged by the plumes and their diameter increase as the plumes descend. Within a linear treatment, as in geophysical work, this model gives the velocity at every section of the plume as a function of distance to the plume axis, and of the distance to its generating level.

However, this model is not applicable to the behaviour of plumes at the boundary. Laboratory experiments (Turner 1986 and references therein) and numerical works (Hulburt et al. 1986, 1994; Asaeda & Imberger 1993) show that vertical currents cross the boundary of the convective region and spread horizontally in a thin penetration layer. That interaction region is strongly non-linear and it is not possible to describe it with

an analytical approach. Even if the numerical simulations (Hulburt et al. 1986, 1994) show the generation of internal waves when the plumes penetrate the stable region, to use these results directly in order to give an analytical definition of our source function is not possible. Some work has been done in astrophysics dealing with the role of such coherent structures in the overshooting (Schmitt et al. 1984; Zahn 1991). The last of these uses a very simple description of plumes and employs the mean horizontal values of fluctuations, and finally gives a parameterization of the depths of the penetration. But, neither these models nor others used in geophysical work are able yet to provide a description of the velocity field at the boundary, where the plumes are stopped by stratification.

Faced with this situation, our only possibility is to approach the problem of the source function from a phenomenological point of view. In fact, the interface between the convective and the radiative zone is disturbed by the currents which arrive at the boundary and beat it as a random function of space and time. The source function, $S(\mathbf{r},t)$, is the superposition of a great number of perturbations with random phase. We can describe the boundary as an undulating surface.

In the following sections we shall present the approached treatments of that problem as it has been used in previous papers, and the improvements introduced here.

2.3. Previous attempts at source function description

We present here the early phenomenological descriptions of internal wave generation used in order to study the diffusion processes linked to the non-adiabatic propagation of these waves in the stellar radiative interior. Press (1981) considered the disturbance at the boundary produced by a turbulent eddy to be described by a $\delta(\mathbf{r},t)$ function, and its effect over the stable region to be a monochromatic oscillation $(\omega,\mathbf{k})$. Furthermore, the properties of this oscillation were determined by an MLT description of turbulent flow in the convective zone. That is, the contributions to the source function came only from eddies with sizes of the order of the mixing length and the horizontal component of the velocity at the boundary given by the mixing length theory of the convective zone:

$$4\pi r_{\rm b}^2 \rho_{\rm b} v^3 = \phi L, \tag{2}$$

where the subscript "b" refers to the bottom of the convective zone, L is the luminosity, and the standard value of ϕ is 0.1. Hence, the horizontal velocity component of a monochromatic oscillation was $u_{\rm H} = v$, horizontal wavenumber $k_{\rm H} = k_{\rm MLT} = 2\pi/\alpha H_{\rm p}$ ($\alpha H_{\rm p}$ is the mixing length), and frequency $\omega = u_{\rm H}/k_{\rm H}$.

The fully developed turbulence in the stellar convective zone is not appropriately described by MLT. In fact, the fluid elements arriving at the boundary of the convective zone present a complete distribution of sizes ($2\pi/k$) and velocities ($v(k)$). García López & Spruit (1991) and Schatzman (1991) assumed that the distribution of turbulent eddies covering the boundary surface could be represented by a Kolmogorov spectrum law $f(k)\,dk = \frac{2}{3}k_{\rm M}^{\frac{2}{3}}k^{-\frac{5}{3}}\,dk$. Where $k_{\rm M}$ is the minimum wavenumber of energy injection, corresponding to the largest scales of convective movement in the framework of MLT ($k_{\rm MLT}$), and where the maximum velocity, $v_{\rm M}$, corresponds to the minimum wavenumber, $k_{\rm M}$, also given by MLT (Eq. 2).

Like Press (1981), these papers consider perturbations as δ functions, and the effects on the other side of the boundary as a set of monochromatic waves with their $(\omega,{\rm k})$ given by the time and horizontal scales of the eddy producing the perturbation. Finally, they adopted the Schwarzschild criterion to define the boundary of convective zone.

Montalbán (1994, hereafter Paper I) also assumed a turbulent flow at the bottom of convective zone described by a Kolmogorov spectrum with the characteristic scales defined by the MLT. Furthermore she introduced two improvements in the treatment of the interaction between convective and radiative zones. Firstly, she took into account Zahn's (1991) model of overshooting, and secondly, she proposed a picture of the disturbed boundary based on Townsend's (1966) model developed to study the same problem in the Earth's atmosphere. In that model a perturbation of the boundary is finite in space and time rather than a $\delta(r,t)$ function, and the oscillation generated in the radiative interior is not a single monochromatic wave, but a superposition of monochromatic waves. The perturbation is described by a derivative of a 1D Gaussian that reproduced the phenomenological description of the convective motion near the boundary (Carruthers & Hunt 1986); that is, a vertical and concentrated motion which becomes completely horizontal when it finds stable stratification. The spatial and temporal characteristic scales of the Gaussian function were given by the size and velocity of eddies generating the perturbation.

In order to test the efficiency of diffusion processes linked to the non-adiabatic propagation of waves generated by those source functions, they compared the theoretical and observational lithium deficiency. The trouble was that, in order to reproduce the observations in F-type stars (García López & Spruit 1991) and in G-type stars (Montalbán 1994; Montalbán & Schatzman 1996), it was necessary to increase the value of parameter ϕ (in Eq. 2) with respect to the value obtained by convection theories and the constraint of thermal equilibrium in the star. The kinetic energy of eddies disturbing the boundary was not high enough. One explanation is that the value of the mean velocity which is derived from the mixing length theory is probably not representative of characteristic velocity of the Kolmogorov spectrum describing the turbulent flow in the stellar convective zone (Schatzman 1991).

They justified the augmentation of vertical velocity as follows: the MLT underestimated the energy of turbulent flow arriving to the bottom of convective zone since, whereas the MLT assumes a symmetry between upward and downward convective motions, numerical simulations and laboratory experiments show that downward motions are much stronger and concentrated than upward ones. Therefore, in order to get an equilibrium state, downward eddies must transport much more kinetic energy than upward ones.

Whereas the general results (García López & Spruit 1991; Montalbán 1994; Montalbán & Schatzman 1996) appeared to

offer an explanation of lithium deficiency, the need for phenomenological adjustment of a basic parameter raised doubts about the model. The picture of convection by plumes given by RZ95 seems to solve that problem. In following sections we give a description of turbulent motion generated in the plume at its arrival at the boundary of the convective zone and the effects over the stable region.

2.4. Plumes and the characterization of turbulence at the boundary

As we have seen above, laboratory experiments and numerical simulations suggest that the plume model of convective heat transport is probably closer to physical reality than bumps. Rieutord & Zahn (1995) developed a simple model of stellar convection by plumes inspired by numerical simulations and experimental data obtained in the Earth's atmosphere. We follow this model in order to characterize the turbulent flow at the boundary of the convective zone, and determine $S(\mathbf{r},t)$. The picture of plumes given by RZ95 seems to solve the difficulties mentioned in the previous section. RZ95 apply the similarity solutions and the linear entrainment hypothesis of Taylor (Turner 1986; Morton et al. 1956) to the stellar case, and conclude that stellar convection can occur though these structures. The number of these structures, imposed by such constraints as thermal equilibrium and geometrical aspects, must be of the order of 1000,

As mentioned above, these solutions are not valid at the boundary in the stratified region; hence, in our approach to the definition of the velocity field in that region we shall take the values of turbulent flow just before the braking location of the plumes. Thus, the similarity solution gives the size of the plume. Its radius b at the bottom of the convective zone of radius $r_{\rm b}$, is equal to

$$b \,=\, \beta_0 (R \,-\, r_{\rm b}) \tag{3}$$

with $\beta_0 \,=\, (6\alpha/7)$, and $\alpha \,=\, 0.083$ (Turner 1986). This gives $b \,=\, 1.45\,10^9$ cm. With a total number of plumes $N_{\rm Pl} \,=\, 1000$ over the whole Sun, it corresponds to a surface occupied by plumes of 0.21 times the solar surface. The maximum vertical velocity of a plume at the bottom of the convective zone is

$$V \,=\, \left(\frac{8(L/N_{\rm Pl})}{\pi \rho_{0\rm b} \beta_0^2 z_0^2}\right)^{\frac{1}{2}} \tag{4}$$

With $\rho_{0\rm b} \,=\, 0.2\,{\rm g\,cm^{-2}}$, the solar luminosity and the thickness of the convective layer ($z_0 \,=\, 2.10^{10}\,{\rm cm}$), we have

$$V \,=\, 2.84\,10^4\,{\rm cm\,s^{-1}}, \tag{5}$$

which is much larger than the value derived from the mixing length theory,

$$V_{\rm MLT} \,=\, \left(\frac{\phi\, L}{4\pi r_{\rm b}^2 \rho_{0\rm b}}\right)^{\frac{1}{3}} \,=\, 3.93\,10^3\,{\rm cm\,s^{-1}} \tag{6}$$

with $\phi = 0.1$. For diving plumes, in order to take into account the effect of sphericity, the self-similar solution of Rieutord and Zahn is modified by introducing correcting terms (Schatzman & Montalbán 1995) for the width of the plumes, their velocity and their density. After integration, this gives for the width

$$b_1 \,=\, 0.92\, b \tag{7}$$

and for the velocity

$$V_1 \,=\, 1.34\, V. \tag{8}$$

Up to now, Eqs. (3 – 8) give the values of mean flow in the plumes. But we need to give here a description of the turbulent motion generated in the plume at its arrival at the boundary of the convective zone. Turbulence is supposed to be generated by the shear flow at the boundary of a plume. We define the boundary as the place where the shear is maximum, $s_1 \,=\, (1/\sqrt{2})b$. We assume that the maximum scale, $b_{\rm M}$, of the turbulence is defined by the place of the maximum velocity gradient. This gives

$$b_{\rm M} \,=\, \left(\frac{e}{2}\right)^{\frac{1}{2}}\, b_1 \tag{9}$$

We can use, to define the characteristic velocity of the turbulent flow, the experimental results on jets mentioned by List (1982):

$$\langle u^2 \rangle^{\frac{1}{2}} \,=\, 0.285\, \langle V \rangle \,\equiv\, V_{\rm M}. \tag{10}$$

We define the average velocity, $V_{\rm av}$, inside the radius of maximum shear,

$$\langle V_{\rm av} \rangle \,=\, \langle V \rangle\, \frac{\int_0^{s_1} \exp(-s^2/b^2) s\, {\rm d}s}{\int_0^{s_1} s {\rm d}s}. \tag{11}$$

2.5. Velocity field in the stable region

As in Paper I we shall analyse here the problem of internal wave generation in the physical frame provided by Zahn's (1991) model of convective penetration. We recall the consequences of that choice over the matter diffusion problem. Firstly, it implies an additional extension of the mixed region, and secondly, it allows us to assume a steep change in the value of the sub-adiabatic gradient, removing at the same time mathematical problems of the boundary conditions. Finally, in order to obtain the velocity field in the radiative zone generated by the disturbed boundary, we shall follow essentially the Fourier treatment proposed by Townsend (1966). With respect to Paper I we introduce two improvements: firstly, we consider a two-dimensional perturbation, and secondly, we shall take into account the random character of the perturbation phenomenon.

In the previous section, we presented a possible description for the velocity field which deforms the interface between the unstable and stable regions. But what is the velocity field generated by the perturbation inside the radiative interior of the star? What is the relationship between the turbulent field and oscillatory movements in the stable region?

With Press's (1981) formulation, the problem is greatly simplified, the forcing is a monochromatic wave, with frequency $\omega_{\rm M}$ and wavenumber $k_{\rm M}$:

$$S(\mathbf{x},t) = u_{\rm M} \exp(i\omega_{\rm M} t + i k_{\rm M} \cdot \mathbf{x}),$$

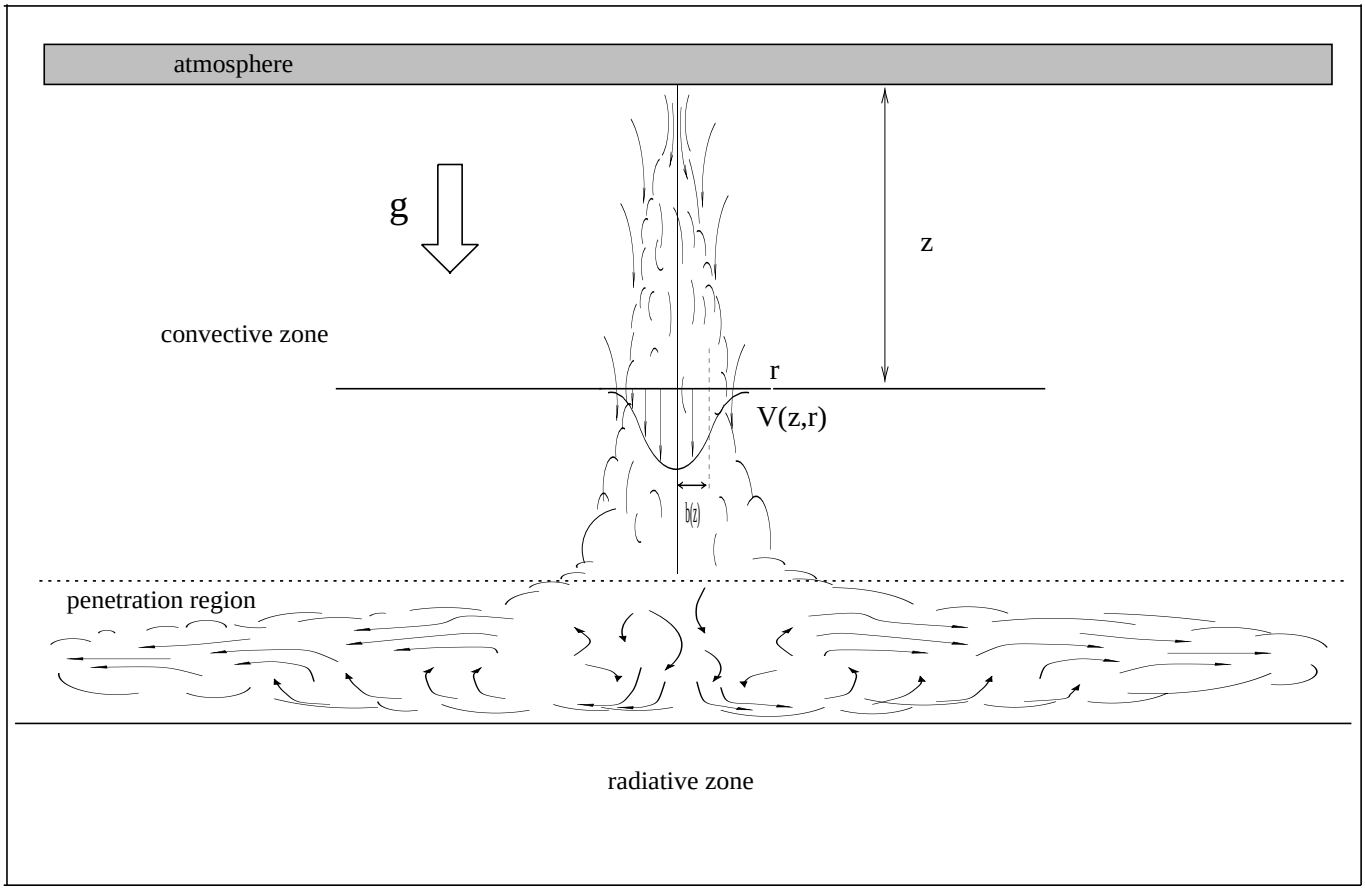

Fig. 1. Phenomenological representation of a plume, based on laboratory experiments (Turner 1986) and numerical simulations (Asaeda & Imberger 1993).

where $\omega_{\rm M}$ and $k_{\rm M}$ become the constants of the movements in the interior. The amplitude of movements in the stable region, according to the boundary constraints imposed by Press, is such that the horizontal component is also $u_{\rm M}$, and the vertical component is given by the dispersion relation and the continuity equation.

As mentioned above, we consider 2D perturbations randomly distributed at the boundary of the convective zone. Hence, the velocity at a point $\mathbf{x}$ and time t is:

$$u(\mathbf{x},t) = \sum_j u_j(\mathbf{x},t) e^{i\phi_j},$$

$$u(\mathbf{x},t) = \int\int\int \hat{u}(\mathbf{k},\omega) e^{(-\imath\mathbf{x}\cdot\mathbf{k}-\imath\omega t)} d\mathbf{k} d\omega.$$

The mean square amplitude of motions at every depth is the number of perturbations by surface and time units, times the amplitude of one perturbation. A perturbation (ξ_0), finite in t and $\mathbf{r}$, can be written as the infinite superposition of monochromatic waves (ω, $\mathbf{k}$), with the coefficients defined by the Fourier transform of the perturbation function ($\mathcal{F}(\xi_0)$). Every one of these monochromatic components propagated according to the expression given by Press (1981) ($\hat{u}_{\rm P}(\omega, k_{\rm H} \mid z)$) is given by:

$$\hat{u}(\mathbf{k}\ ,\ \omega, z) \sim \hat{u}_{\rm H}(\mathbf{k},\omega,z_b) \frac{|\omega|}{N_b} \left(\frac{r_b}{r}\right)^{\frac{3}{2}} \left(\frac{\rho_b}{\rho}\right)^{\frac{1}{2}} \left(\frac{(N^2/\omega^2-1)^{-\frac{1}{4}}}{(N_b^2/\omega^2-1)^{-\frac{1}{4}}}\right) \exp\left(-\frac{1}{2} f \frac{k^3}{\omega^4}\right) e^{-\imath(\mathbf{k}\cdot\mathbf{r}+\omega t)}. \quad (12)$$

where f represents the part of the damping depending only on the depth below the boundary of the convective zone; N is the Brunt–Väisälä frequency, and the indices b refers to the bottom of the convective zone.

At every depth z the velocity field in the real domain $(\mathbf{x}, t)$ is given by the inverse Fourier transform.

Boundary disturbance by an eddy can be assimilated to a Gaussian function of space and time. An eddy of size $2\pi/k = b$ arriving at the boundary with a velocity $u_{\rm b}$ will generate a perturbation that we can express as:

$$\xi_0(x,y,t \mid z=0) = u_{\rm b} \exp\left(-\frac{1}{2}\left(\frac{q^2}{b^2}+\frac{t^2}{\tau^2}\right)\right) \quad (13)$$

where $q^2 = x^2 + y^2$ is the horizontal component, τ is the characteristic time scale for the perturbation and b is the characteristic dimension of turbulent element of fluid producing the perturbation.

In Fourier space,

$$\xi_0 \implies \mathcal{F}(\xi_0(\mathbf{q},t))(\mathbf{k},\omega)$$

where

$$\mathbf{q}=(x,y) \quad \text{and} \quad \mathbf{k}_{\rm H}=(k_x,k_y).$$

Since we suppose that the perturbation has circular symmetry, the relationship between the components in the real space and in the Fourier space are given by the following expressions: ($x = q\cos\theta; y = q\sin\theta; t$) and ($k_x = \ell\cos\varphi; k_y = \ell\sin\varphi; \omega$). The Fourier transform[1] of the perturbation ξ_0 is

$$\begin{aligned}\mathcal{F}(\xi_0)(\ell,\omega) &= \frac{u_{\rm b}}{\sqrt{2\pi}}\int_{-\infty}^{\infty}\exp\left(-\frac{1}{2}\frac{t^2}{\tau^2}\right)\exp(-i\omega t)dt \\ &\quad \int_0^{\infty}\exp\left(-\frac{1}{2}\frac{q^2}{b^2}\right)J_0(\ell q)qdq \\ &= u_{\rm b}\tau b^2\exp\left(-\frac{1}{2}\left(\ell^2b^2+\omega^2\tau^2\right)\right). \end{aligned} \tag{14}$$

This expression is a splitting into harmonics (ω,ℓ) of a perturbation with space characteristic scale b, and period τ. The velocity field at a point in the radiative zone is the result of contributions from several perturbations with the same spatial scale which arrive at different points of the boundary, and from a complete distribution of sizes. At a depth z below the source, the contribution to the harmonic (ω, ℓ) provided by a perturbation in $r = 0$ at $t = 0$, is

$$\mathcal{F}(\xi_0)(\ell,\omega)\cdot\hat{u}_{\rm P}(\ell,\omega \mid z);$$

so that the effect from perturbations arriving at different points $\mathbf{q}_{\rm j}$ and at different times $t_{\rm j}$, is

$$\begin{aligned}\mathcal{F}(\xi_{\rm j}) &= \int\int \xi_0(\mathbf{q}-\mathbf{q}_{\rm j},t-t_{\rm j})e^{-i\omega t}e^{-i\mathbf{q}\cdot\mathbf{k}}d\mathbf{q}dt \\ &= e^{-i\omega t_{\rm j}}e^{-i\mathbf{q}_{\rm j}\cdot\mathbf{k}}\mathcal{F}(\xi_0).\end{aligned}$$

The harmonic (ℓ,ω) due to $N_{\rm p}$ perturbations is the incoherent superposition of every one of these perturbations. Then,

$$u(\mathbf{q},t)=\sum_i u_i(\mathbf{q},t) \tag{15}$$

$$\hat{u}(\mathbf{k},\omega)=\sum_i \hat{u}_i(\mathbf{k},\omega) \tag{16}$$

$$\begin{aligned}\hat{u}(\ell,\omega) &= \sum_{j=1}^{N_{\rm p}} e^{-i\omega t_{\rm j}}e^{-i\mathbf{q}_{\rm j}\cdot\mathbf{k}}\mathcal{F}(\xi_0)(\ell,\omega)\hat{u}_{\rm P}(\ell,\omega|z) \\ &= \mathcal{F}(\xi_0)(\ell,\omega)\hat{u}_{\rm P}(\ell,\omega|z)\left\{\sum_{j=1}^{N_{\rm p}} e^{-i\omega t_{\rm j}}e^{-i\mathbf{q}_{\rm j}\cdot\mathbf{k}}\right\}\end{aligned} \tag{17}$$

[1] Symmetric definitions of Fourier Transform:

$$f(\omega)=\frac{1}{\sqrt{2\pi}}\int_{-\infty}^{\infty}F(t)e^{-i\omega t}dt.$$

In real space, the velocity $u(\mathbf{q},t \mid z)$ is the inverse Fourier transform of $\hat{u}(\ell,\omega \mid z)$. The amplitude of the mean square velocity (uu^*) is:

$$\langle u^2\rangle = \frac{1}{\Sigma.t}\int_{-\infty}^{\infty}\int_{-\infty}^{\infty} \mid u(\mathbf{q},t \mid z)\mid^2 d\mathbf{q}dt, \tag{18}$$

where Σ is the integration area. As we consider axisymmetry:

$$\langle u^2\rangle = \frac{2\pi}{\Sigma.t}\int_{-\infty}^{\infty}\int_{0}^{\infty} \mid u(q,t \mid z)\mid^2 qdq\,dt, \tag{19}$$

and by the Parseval's or Rayleigh's theorem

$$\begin{aligned}&\int_{-\infty}^{\infty}\int_{0}^{\infty} \mid u(q,t \mid z)\mid^2 qdq\,dt = \\ &\qquad \int_{-\infty}^{\infty}\int_{0}^{\infty} \mid \hat{u}(\ell,\omega \mid z)\mid^2 \ell d\ell\,d\omega.\end{aligned} \tag{20}$$

According to Eq. (17),

$$\begin{aligned}\mid \hat{u}(\ell,\omega \mid z)\mid^2 &= \hat{u}(\ell,\omega \mid z)\cdot\hat{u}^*(\ell,\omega \mid z) \\ &= \mid \mathcal{F}(\xi_0)\mid^2 \cdot \mid \hat{u}_{\rm P}(\ell,\omega \mid z)\mid^2 \\ &\quad \cdot \left\{\sum_{j=1}^{N_{\rm p}} e^{-i\omega t_{\rm j}}e^{-i\mathbf{q}_{\rm j}\cdot\mathbf{k}}\right\}\left\{\sum_{j=1}^{N_{\rm p}} e^{+i\omega t_{\rm j}}e^{+i\mathbf{q}_{\rm j}\cdot\mathbf{k}}\right\}.\end{aligned} \tag{21}$$

The terms inside the keys are equivalent to:

$$N_{\rm p}+\sum_{j\neq n}^{N_{\rm p}} e^{i(\phi_n-\phi_j)} \longrightarrow N_{\rm p},$$

where $N_{\rm p}$ is the number of Gaussian perturbations with characteristic spatial dimension b. As the number of perturbations is very large, and we consider that they are randomly distributed, the incoherent superposition of harmonics will make the second summation disappear. It then turns out that

$$\mid \hat{u}(\ell,\omega \mid z)\mid^2 = N_{\rm p}\mid \mathcal{F}(\xi_0)\mid^2 \cdot \mid \hat{u}_{\rm P}(\ell,\omega \mid z)\mid^2. \tag{22}$$

Introducing the expression (Eq. 12) for the vertical velocity of a monochromatic wave,

$$\mid \hat{u}_{\rm P}(\ell,\omega \mid z)\mid^2 = \Phi^2(r)\exp\left(-\frac{\ell^3}{\omega^4}f(z)\right), \tag{23}$$

Eqs. (19), (22) and (21), lead to:

$$\begin{aligned}\langle u^2\rangle &= \frac{2\pi}{\Sigma\cdot t}N_{\rm p}(\tau b^2)^2u_{\rm b}^2\Phi^2(r) \\ &\quad \int_{-\infty}^{\infty}\int_{0}^{\infty}\exp\left(-\ell^2b^2-\omega^2\tau^2-\frac{\ell^3}{\omega^4}f(z)\right)\ell d\ell d\omega,\end{aligned} \tag{24}$$

where $\Phi(r)$ contains the whole dependence on r.

The number of perturbations per unit of time at the boundary of the convective zone, according to the chosen framework (Sect. 2.4), is given by the plume dimensions. We consider that the number of perturbations with dimension b can be given by

$$N_{\rm p}=N_{\rm Pl}\left(\frac{b_{\rm M}}{b}\right)^2, \tag{25}$$

where $N_{\rm Pl}$ is the global number of plumes. Then, taking into account the boundary conditions described above, we know the mean square velocity on the turbulent side, but we do not know the velocity at the other side of the boundary. The eddies have a velocity $u_{\rm T} \equiv u_{\rm b}$, whereas the waves generated by these eddies have an amplitude $u_{\rm H}$, and a random distribution of phase. As Chandrasekhar (1943), Rayleigh (1899–1920) and García López & Spruit (1991) have pointed out, because of the interferences of white noise, the mean square value of the wave velocity is related to the square value of the white noise source by:

$$\langle u_{\rm H} \rangle^2 = \frac{1}{n_{\rm eddies}} u_{\rm T}^2,$$

where $n_{\rm eddies}$ is the number of eddies at the boundary contribution to one wave number, (ℓ); this number is of order $(\ell_{\rm M}/\ell)^2$. Then, going from turbulent to oscillatory movement, the effect is the diminution by a factor $(\ell/\ell_{\rm M})^{-2}$ of the mean square amplitude:

$$\mid u_{\rm H}(x,t) \mid^2 = \langle \hat{u}_{\rm T}(\ell,\omega) \rangle^2 \left(\frac{\ell}{\ell_{\rm M}} \right)^{-2}. \quad (26)$$

In order to compute the integral (Eq. 24), we take the approximation,

$$\frac{\tau^4}{b^3} f(z) \gg 1.$$

This corresponds to a damping such that $f \gg 10^3$. In the Sun, this value is reached at 2.10^6 cm beneath the convective region. That means that the approximation is already valid very close to the boundary where internal waves are excited.

The expression for the mean square value of vertical velocity at any depth, z, due to the contribution from all of perturbations with size b is

$$\langle u^2 \rangle = \frac{1}{6} \Gamma(11/6) \Gamma(2/3) \frac{N_{\rm Pl}}{N^2} u_{\rm H}^2 \Phi^2(r) \frac{b_{\rm M}^2}{r_{\rm b}^2} \frac{b^4}{\tau^4} f^{-2/3}(z). \quad (27)$$

3. Diffusion coefficient

The diffusion process we are dealing with is linked to the non-adiabatic propagation of internal waves in the stellar radiative interior. As explained by Press (1981), when the thermometric diffusivity is zero, the diffusive transport is entirely horizontal (Bretherton 1969; Grimshaw 1972; McIntyre 1973). There is no vertical diffusive transport as the fluid entropy carries a memory of the level at which it should sink or rise, counteracting any second-order fluid forces. However, irreversible effects due to dissipative processes such as radiative damping, generate a finite r.m.s. displacement of fluid elements. A diffusive process takes place.

Schatzman (1991) assumes that it is possible to define the contribution to the macroscopic diffusion coefficient due to an internal wave ($\omega, k_{\rm H}$) that propagates in a dissipative medium ($D_{\rm th}$ is the thermometric diffusivity), as the product of a length (the distance reached by a fluid element after an overturn ω^{-1}):

$$l_{\rm D} \sim D_{\rm th} N \frac{k_{\rm H}^3}{\omega^4} u_{\rm Hb}^2 . \frac{u_{\rm V}^2}{u_{\rm Vb}^2}, \quad (28)$$

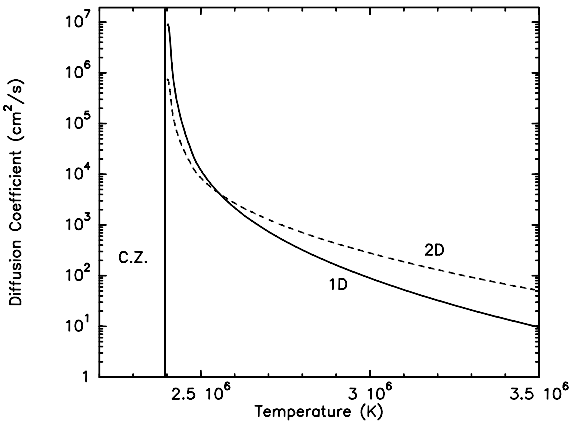

Fig. 2. Diffusion coefficient as a function of temperature down the bottom of the convective envelope for a solar model. 1D corresponds to Paper I treatment, Eq. 29 with n=1; and 2D corresponds to the plume approximation, Eq. 29, with n=2/3.

and a velocity (the product of the distance by the circular frequency, $v_{\rm D} = l_{\rm D} \cdot \omega$). N is the Brunt–Väisälä frequency, $u_{\rm V}^2$ is the vertical velocity of the wave at each depth in the radiative zone, and $u_{\rm Vb}^2$ is the same at the boundary of the convective zone. $u_{\rm Hb}^2$ is the horizontal component of the velocity produced by the turbulence at the boundary of the convective zone. To derive the total diffusion coefficient involves the integration over the spectrum of the turbulence in order to take into account the contribution to the diffusion process from all the scales.

We follow here the same procedure as in Paper I; that is, we substitute the square value of the amplitude of monochromatic waves by the mean square velocity in the radiative interior (Eq. 27). After integrating over the spectrum of turbulence, the diffusion coefficient derived is:

$$D_{\rm Mix} = A \left\{ D_{\rm th} N \left(\frac{\rho_{\rm b}}{\rho} \right) \left(\frac{r_{\rm b}}{r} \right)^6 \right\}^2 b_{\rm M}^{1-2n} V_{\rm M}^{8n-3} f^{-2n}, \quad (29)$$

where $n = 2/3$. Comparing with 1D description of perturbation (Paper I), the diffusion coefficient has a similar expression, but with $n = 1$. A is a numerical factor coming from the integration. In the 1D formulation its value is of the order of 0.1, and in the present case (2D) A contains also the number of plumes, and for 1000 plumes its value is of the order of 8.10^{-2}.

Therefore, the diffusion coefficient is composed of four terms: a numeric factor (A), a term containing dependence on radius, a term containing the features of turbulent flow at the bottom of the convective zone (V_M and b_M), and finally, a term containing the radiative damping effect (f), depending on the depth below the convective zone.

In Fig. 2 we plot both diffusion coefficients (1D and 2D) for the Sun. We observe that the new one decreases less rapidly than the Paper I diffusion coefficient.

On the other hand, we are aware that we should introduce our Gaussian disturbance into the computation of the mean square displacement representing the perturbation by a Fourier series (Schatzman & Montalbán 1995; Schatzman 1996). The method that we use implies that the damping effect is considered as an

average, linking to every Gaussian perturbation with size b and period τ the damping corresponding to a monochromatic wave with wave number $1/b$ and frequency $1/\tau$. However, results following a more correct mathematical treatment are not very different (Schatzman 1996).

4. Results and discussion

In this section we present the predictions of lithium and beryllium abundance given by the diffusion process presented in previous sections. We analyse the dependences of atmospheric abundances of these elements on age and mass, and we compare these theoretical results with observational data of Li in open clusters, and Be in open clusters and field stars. We also propose a possible explanation of lithium abundance spread in the framework of the internal wave diffusion process. We discuss the role of interaction convection/rotation on the source of internal waves, and hence on the chemical diffusion process.

4.1. Stellar models

The internal structure of the stars used in the computation of the light element abundances has been determined using the stellar evolution code CESAM developed by Morel (1992). Opacity data were taken from OPAL opacity tables (Rogers & Iglesias 1992), completed with LOAL (Los Alamos Opacity Tables, Huebner et al. 1977) at high temperature, and with Kurucz (1991) for temperatures lower than 10^4 K. These tables have been compiled from the Anders & Grevesse (1989) meteoritic composition.

Models have been computed with solar chemical composition ($Z = 0.0194$). The value of $X = 0.678$ is given by calibrating the $1\,\mathrm{M}_\odot$ model with the Sun. We have computed a sequence of models with effective temperatures ranging between 6200 K and 4000 K. These models were obtained following the evolution from an initial homogeneous model to the ages 1.10^8, 3.10^8, 5.10^8, 8.10^8, 1.10^9, 2.10^9, 3.10^9 and $4.5.10^9$ yr.

The convective zone has been calculated with a mixing length parameter $\alpha = 1.79$ given by the solar calibration, and we also introduce the convective penetration at the bottom of the convective stellar envelope as modelled by Zahn (1991). In this model the depth of penetration is given by $L_\mathrm{p} = \zeta H_\mathrm{p}/\chi_\mathrm{p}$, where χ_p is the gradient of the conductivity at the boundary, H_p is the pressure scale height, and ζ is a parameter that gives an idea of the ratio of the convective efficiency in the unstable and stable regions. We use $\zeta = 0.5$, in agreement with helioseismological measures (Berthomieu et al. 1993) also based on a solar model computed with the same version of the CESAM code. We have also computed calibrated stellar models with $\zeta = 0.25$ for solar chemical composition and ages $1.10^8, 3.10^8, 5.10^8$ and 8.10^8 yr.

In order to determine the light elements abundances, we solve the diffusion equation for every stellar model (at each value of mass and age) employing the method of eigenvalues described by Baglin et al. (1985).

4.2. Lithium depletion rate as a function of mass and age

The lithium depletion observed on the stellar surface suggests that either the temperature at the bottom of the convective envelope is higher than the lithium burning temperature ($\mathrm{T_{Li}} \approx 2.5 10^6$ K), or that this element is by some means transported out of the convective zone and, since in this region the matter is completely mixed, the observed effect is an effective reduction in the lithium concentration at the surface.

Lithium abundance depends on several physical parameters as we have noted above. To analyse the dependence on mass and the age of lithium depletion, lithium observations in open clusters are usually employed. These associations are supposed to have the same chemical composition and age; therefore, differences in lithium abundance must be due only to the spectral type. On the other hand, to compare lithium observations in open clusters with different ages allows an analysis to be made of the influence of age. Both, the smooth decrease of Li with spectral type (Cayrel et al. 1984) and lithium evolution with time show that in solar-type stars the lithium is transported slowly.

The lithium abundance observed at a given age is a measure of the time that the transport mechanism requires to drive matter from the bottom of the convective zone to the combustion layer. This distance between both layers (z_Li) depends on the age of the star and on the spectral type. The depth of convective envelope increases as the mass decreases. Since the diffusion coefficient decreases very quickly with depth, the diffusion time rises significantly. Therefore, the lower the stellar mass, the higher the efficiency of the transport process and the lower the lithium abundance. These aspects are well reproduced by our transport process: in Fig. 3 we can see that for lower-mass stars the lithium depletion is much more important at every age. That lithium depletion in the low-mass main sequence is clearly observed in the Hyades cluster (Cayrel et al. 1984; Thorburn et al. 1993), where at 8.10^8 yr, a star with 0.7 $\mathrm{M}_\odot$ has depleted its original content of lithium (we assume 3.2 in the log(Li/H)+12 scale) by a factor 200, whereas a solar mass star is only depleted in a factor 10.

Furthermore, for a main sequence star with a given mass, the older the star, the shallower its convective zone. If the temperature at the bottom of the mixed envelope decreases, then the distance to the Li-burning layer increases. Therefore, the efficiency of the transport mechanism decreases as the age increases. Thus, the lithium depletion rate has decreased by 60% between 8.10^8 and 5.10^9yr. That is also reflected observationally when we compare the lithium depletion in Hyades solar-type stars, and the depletion 4.10^9 yr later in the old cluster M 67.

We shall test the ability of the internal wave diffusion process to explain the dependence of lithium abundance on spectral type and age, comparing the predictions of our diffusion process with the observations in some open clusters: UMa (Soderblom et al. 1993a), M 34 (Jones et al. 1997) and NGC 6475 (James & Jeffries 1997), 3–5.10^8 yr; Praesepe (Soderblom et al. 1993c), Hyades (Balachandran 1995) and NGC 6633 (Jeffries 1997),

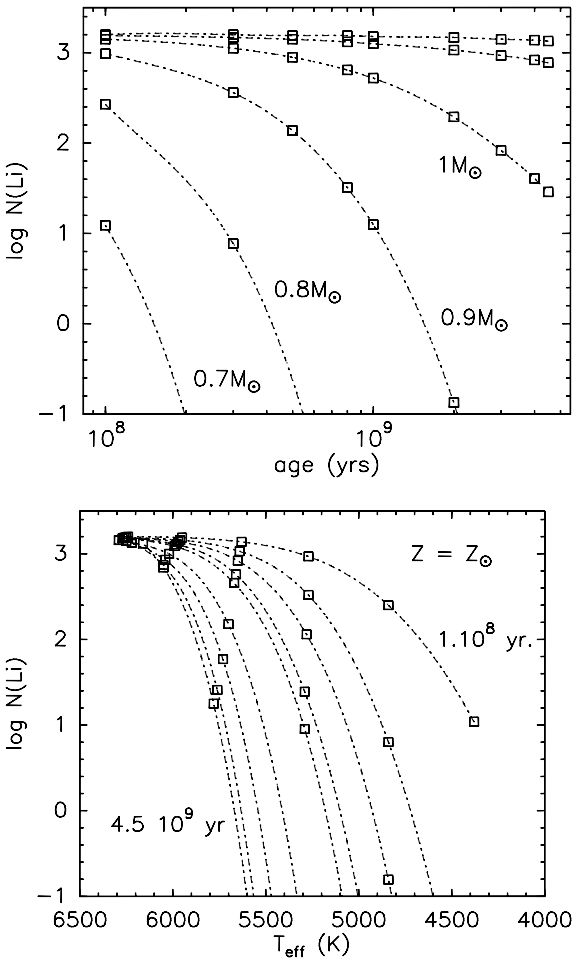

Fig. 3. Upper panel: each curve shows the Li abundance evolution for a given mass (0.7, 0.8, 0.9, 1.0, 1.1 and 1.2 $M_\odot$) as predicted by the diffusion coefficient in Eq. (29). Points mark the computed stellar models. Lower panel: Li versus $T_{\rm eff}$ curves predicted by Eq. (29). We plot the curves at the ages 1.10^8 yr (the Pleiades by Soderblom et al. 1993b), 3.10^8, 5.10^8, 8.10^8, 1.10^9, 2.10^9, 3.10^9, 4.10^9 and 4.5 10^9 yr.

8.10^8 yr; NGC 752, 2.10^9 yr; and M 67, 5.10^9 yr (Balachandran 1995; Pasquini et al. 1997).

As we have explained above, our models begin by being homogeneous. For the mass range considered here, it is shown that these models for ages $\geq 10^8$ yr are equivalent to those which should be obtained following the PMS evolution. However, we cannot determine what the contribution is from our diffusive process between 0 and 10^8 yr. Since the distance between the bottom of the convective zone and the lithium-burning layer changes as the star evolves, we cannot simply extrapolate the value of the lithium depletion rate at 10^8 yr ($\lambda_{\rm Li}(10^8)$) till $t = 0$. This will not be too bad for low-mass stars because at 10^8 yr or for earlier ages, the bottom of their convective zone is hot enough to burn lithium. But for more massive stars the temperature at the bottom of the convective zone is high enough to burn lithium during the PMS, decreases as the star approaches the mean sequence, and is lower than $T_{\rm Li}$ at 10^8 yr. Therefore, extrapolating the $\lambda_{\rm Li}(10^8)$ to earlier ages we should obtain a lower limit for lithium depletion.

In Paper II we took the D'Antona & Mazzitelli's (1994) values for the PMS lithium depletion, but comparing with the Pleiades observations, García López et al. (1994) showed that these models depleted too much lithium in low-mass stars. So, we use as a value at 10^8 yr the observational lithium obtained in the Pleiades by Soderblom et al. (1993b). Given the large spread in these measurements we have taken a lower and an upper envelope of those data. Thus, in each figure, there are for each set of parameters a couple of curves corresponding to the upper and lower envelopes as initial values, and the curves corresponding to 10^8 yr are exactly those chosen for the Pleiades. From these curves we take into account the contribution of the internal wave diffusion mechanism, integrating the lithium depletion rate at each time from $t = 10^8$ to the age considered.

In Fig. 4 we present the results of that comparison. In panel **a)** we plot the lithium abundances in young clusters with ages between 2 and 3.10^8 yr. M 34 (Jones et al. 1997), which is 250 Myr old, is represented by circles. NGC 6475 (James & Jeffries 1997) is 220 Myr old and is represented by triangles. The observational values for Ursa Major (3.10^8 yr) are taken from Soderblom et al. (1993a) and are represented by squares (in all cases, empty symbols represent upper limits). The plotted curves correspond to theoretical results for 3.10^8 yr. There are two pairs of curves computed by considering two different values of the overshooting parameter ($\zeta = 0.5$ and $\zeta = 0.25$). These choices will be discussed in the next section when considering the effects of stellar rotation on overshooting (higher rotation, less overshooting). In these curves we see that the effect of different overshooting is significant for low-mass stars and is almost negligible for solar-mass stars, increasing the spread in lithium abundance at the low-mass end. This is explained by the fact that for low-mass stars the bottom of the convective zone is close to the lithium-burning layer, and a relatively small change in its location implies moving the boundary of the mixed region below the $T_{\rm Li}$ layer, and so an important depletion of atmospheric abundance of lithium occurs. To plot also the curves corresponding to no additional transport process would produce a really overcrowded graph, but we can say that if we also join these curves we see that the whole set of six curves perfectly enclose the observational data. For such early ages, the convergent behaviour of different curves with and without transport processes is explained because the diffusion process is slow and has not worked long enough to produce a large depletion of lithium. However, non-diffusion curves will be well separated from diffusion curves when older models and clusters are considered.

Close to 4500 K there is a group of stars that is clearly above the curve predicted by the mixing process (but near the curve without mixing). We can consider several aspects that might affect the position of these stars in the diagram. First, most of these stars belong to M 34 and two of them to NGC 6475; these clusters are a little younger than 300 Myr. Second, in this range of masses the effect of a small change in the overshooting is quite significant. Furthermore, the stars in M 34 all have

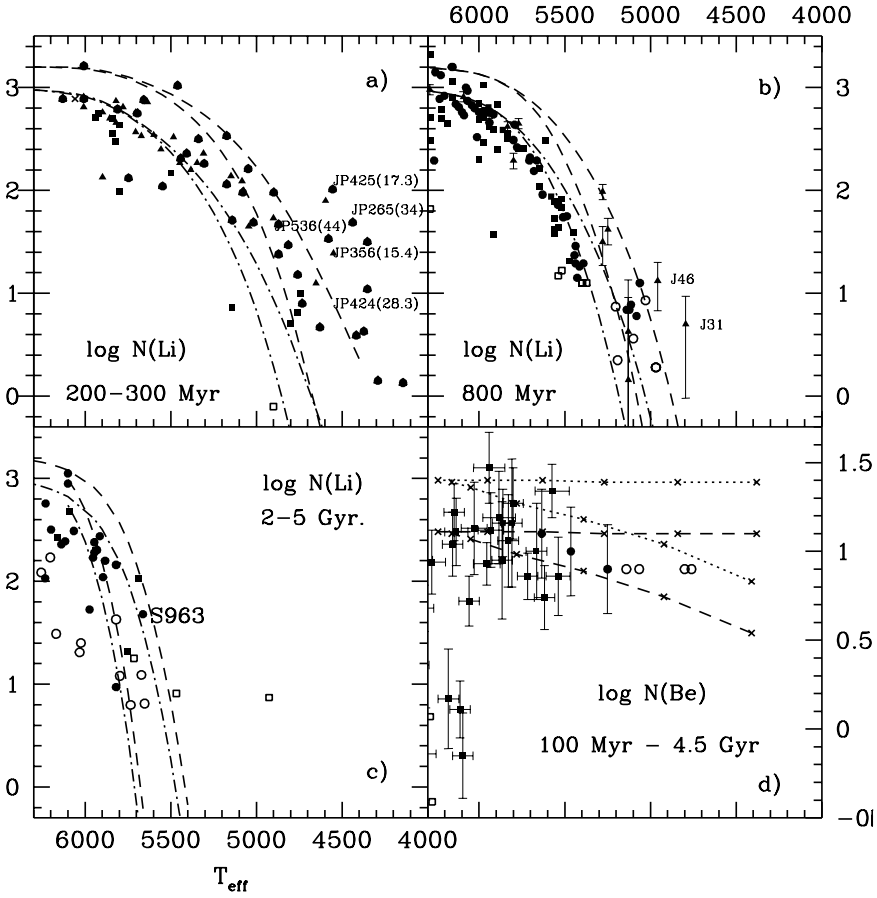

Fig. 4. **a** Lithium abundance predicted at 3.10^8 yr for models with two different values of overshooting ($\zeta = 0.25$ and $\zeta = 0.5$) and observational data for NGC 6475 (triangles) 220 Myr old, Ursa Major (squares) and M 34 (circles) 3.10^8 yr old. Upper curves (dashed lines) correspond to abundances evolved from the upper envelope in the Pleiades, and lower curves (dash-dotted lines) to the abundance evolved from the lower envelope in the Pleiades. **b** The same than panel **a**, but at 810^8 yr. Observational data for the Hyades (circles) and Praesepe (square) from Balachandran (1995), 8.10^8 yr old, and for NGC 6633 (triangles) 600–650Myr old. **c** Lithium abundance predicted at 2.10^9 yr (upper curves) and at 4.510^9 yr (lower curves) for models with overshooting $\zeta = 0.5$. Observational points for NGC 752 (squares) $\approx 2.10^9$ yr old (Balachandran 1995); and M 67 (circles) 4.7–5.10^9 yr old from Balachandran (1995) and Pasquini et al. (1997). **d** Beryllium abundance at 1.10^8 and 4.510^9 yr predicted by Eq. (30), taking as initial beryllium abundances 1.42 (dotted lines) and 1.11 (dashed lines). Crosses mark the computed models. Observational points for the Hyades and Ursa Major Group (circles) from García López et al. (1995), and for field stars (squares) from Stephens et al. (1997). Empty symbols represent upper limits.

$v \sin i > 15\,\mathrm{km\,s^{-1}}$; consequently, overshooting in those stars can be much less efficient (Sect. 4.3). In the figure we have written the identifier and $v \sin i$ value for each in brackets. Finally, only JP425 is a member of the cluster with a probability greater than 60% (JP425, 75%; JP265 53%; JP536, 48%; JP356, 18% and JP424, 46%).

In panel **b)** we show the theoretical results for 800 Myr (as in panel **a)** there are two pairs of curves corresponding to different values of overshooting) and the observational data for the Hyades (circles) and Praesepe (squares) from Balachandran (1995), both $\approx$ 800 Myr old (Strobel 1991); and NGC 6633 (triangles) from Jeffries (1997). The last one is slightly younger, 600–650 Myr (Strobel 1991; Janes et al. 1988). There is also a difference in the metallicity of these clusters, Jeffries (1997) estimates that NGC 6633 has a significantly lower metallicity than the Hyades (+0.12), but it cannot be much less than solar, he estimates that [M/H] must be between –0.1 and +0.05, close to the Pleiades metallicity. To analyse these results, we must keep in mind these differences in age and chemical composition and two further facts: first, that all our stellar models have been computed with solar composition; and second that we took as lithium abundance at 10^8 yr the observational data in the Pleiades, with slightly sub-solar metallicity (-0.034 ± 0.024 Boesggard & Friel 1990). We recall that decreasing the metallicity results in shallower convective regions and the cooler bottom layer of the convective zone, and that these differences in metallicity could have a large influence on the lithium depletion rate throughout the PMS of low mass-stars. So the difference in metallicity could produce a different Li depletion at 10^8 yr for the Hyades and Pleiades. In the figure there are two stars in NGC 6633 that are clearly well above the theoretical curves. However, we must take various aspects of the problem into account. First, if we plot the theoretical curves corresponding to lower age, 5.10^8 yr, the points classified as detections by Jeffries (1997) are below the curve. However, in order to invoke this solution it would be necessary to have data between 5200 and 5900 K. Second, as we note above, in the case of low masses, the effect of a slightly different value for the overshooting parameter could be significantly high. Jeffries (1997) provides only upper limits for the rotational velocity of these stars, so we cannot invoke a high velocity as an explanation for the high lithium content.

Finally, in panel **c)** we plot the data belonging to two old clusters, NGC 752 (2.10^9 yr, Strobel 1991) and M 67 (4.7–5 10^9 yr, Hoobs & Pilachowski 1986), both with solar metallicity. The curves traced correspond to models with 2.10^9 and 4.5 10^9 yr, and for a single value of the overshooting ($\zeta = 0.5$). In comparing with the other panels we see that for effective temperatures larger than 5500 K the effect of different overshooting depths is not very significant. For NGC 752 the observational points (squares) in the mass range of interest are very scarce and spread. We can only say that they are not incompatible with the theoretical curves. The data for M 67 (circles) are taken from Balachan-

dran (1995) and from Pasquini et al. (1997). This cluster is also well known for the large dispersion in lithium abundances for the same colour. Most of the stars have evolved away from the mean sequence and are generally very weak objects. Pasquini estimates an error in the effective temperature determination of the order of 150 K. There is one object (S963) that clearly does not fit the theoretical predictions. From the literature we know only that it is a binary with magnitude $V = 14.5$. An error of 150 K in $T_{\rm eff}$ could bring the star closer to the predictions, but there are insufficient data on this star for analysing its role in our problem.

4.3. Lithium abundance dispersion: the role of rotation

Lithium depletion in the framework of our model is strongly related with the overshooting of convective motions in the stable stratification region; first because it implies a supplementary extension of the mixed region and second because convective overshooting of turbulent flows in stable region excites the internal waves which propagate inside the radiative region producing the diffusion process. In the description of the model (Sect. 2) we do not consider stellar rotation, which could, however, have significant effects on both i) the source function of internal waves due to the influence of rotation on convective motions, and ii) the propagation of internal waves due to the change in the dispersion relation in a rotating frame.

Concerning internal wave propagation in a rotating frame, the dispersion equation relating the horizontal and vertical wave number must be change from $k_{\rm V} = k_{\rm H}(1 - N^2/\omega^2)^{1/2}$ used in the derivation of the velocity (Eq. 12), to (see, Unno et al. 1989)

$$k_{\rm V} \simeq \frac{k_{\rm H}}{\omega^2 - 4\Omega^2 \sin^2\phi} \left(2\Omega^2 \sin 2\phi \pm (-\omega^4 + \omega^2(N^2 + 4\Omega^2) - 4N^2\Omega^2 \sin^2\phi)^{\frac{1}{2}}\right), \quad (30)$$

where Ω is the angular velocity and ϕ is the latitude.

Since the WKBJ solution of the wave propagation equation is proportional to $(k_{\rm V})^{-1/2}\ \exp(ik_{\rm V}\cdot z)$, the constraint on the frequencies propagating can be expressed as

$$N^2\left(1 + \frac{4\Omega^2}{N^2}\cos^2\phi\right) > \omega^2 > 4\Omega^2 \sin^2\phi. \quad (31)$$

Thus, the horizontal component of the rotation vector has as an effect that increases the strength of the stratification, but it does not seem significant. For a solar-type star, rotating at 30 km s^{-1} (which is quite high) the factor $4\Omega^2/N^2$ is of the order of 7.10^{-3}. The vertical component of the rotation vector constrains the minimum frequency that can be propagated. That effect is null at the equator and maximum at the pole, and for the example given above, only waves with frequency higher than $8.10^{-5}{\rm s}^{-1}$ will be able to propagate. So, the effect of rotation is to provide a cut-off at the lower end of the internal wave spectrum. The cut-off frequency increases as the vertical component of the rotation vector increases. On the other hand, we recall that the radiative damping of internal waves is proportional to ω^{-4}; therefore, the frequencies that are affected by the cut-off are (except for high rotation velocity) also those that should not penetrate very deeply in the stable region.

A quantitative estimate of the effect of rotation on the diffusion coefficient is beyond the scope of this paper. However, the previous paragraphs indicate that the effect of rotation averaged over the sphere should reduce the efficiency of the transport processes due to the propagation of internal waves.

Concerning the source function, it seems that in non-rotating turbulent compressible convection the motions in the interior are vertically coherent, large vortices crossing the greater part of the domain and co-existing with small-scale vortex tubes. But the effects of rotation could modify these characteristics of turbulence. Numerical simulations of convection constrained by rotation have been carried out by Julien et al. (1996b, 1997b) in the incompressible approximation and considering rotation vector parallel to gravity, and by Brummell et al. (1996) in the compressible case and taking into account different angles between gravity and rotation. These papers, studying the effects of rotation on turbulence in the interior of the convective zone, show a subtle modification of turbulence characteristics as a function of the Coriolis force. Julien et al. (1996a) discuss some preliminary results from 3D numerical simulations of incompressible penetrative convection in the presence of rotation. Their results make it clear that rotation can significantly alter the mean properties of the convective mixed layer and the penetration layer. Julien et al. (1997a) suggest that these results could be relevant to a statistically steady configuration of the Sun, since many of the key effects of rotation observed in the non-penetrative case (Julien et al. 1996b; Brummell et al. 1996) are also observed in the penetrative case, e.g. enhancement of lateral mixing due to vortical thermal plume interactions and sustained unstable thermal stratification. The effects of rotation should therefore be taken into consideration in estimating the extent of overshooting beyond the base of the solar convective zone.

Numerical simulations with and without rotation reveal striking differences in the plume structure in non-rotating and rotating flows. Without rotation, a few strong plumes extend into the mixed layer. Encountering the stably stratified region below, plumes penetrate deeply into this region. Fluid is carried into the mixed layer through vigorous up-welling around the plumes, providing evidence for the transport of fluid in the stable stratified region below. In contrast, at high rotation, the rotation strongly reduces the length scales of the plumes and by the association of plumes with cyclonic vertical vortices, the mixing properties are altered. Interaction between such cyclonic structures result in a strong stirring and lateral mixing of temperature, diluting the buoyancy anomaly of the plumes (Julien et al. 1996b, 1997b; Brummell et al. 1996). The vertical transport of bouyancy is therefore reduced indicating an equivalent reduction of fluid transport in the stably stratified region. Furthermore, the plumes which reach the bottom of the mixed layer are small and weak, their horizontal dimensions increasing little with depth, unlike the non-rotating case.

There are great differences in the instantaneous kinetic energy budgets for the rotating and non-rotating case. Whereas

the buoyant production term is approximately unchanged in the upper part of the mixed layer, at high rotation the dissipation of kinetic energy is larger due to lateral mixing, and the transport of kinetic energy out of the upper part of the mixed layer is correspondingly smaller.

Furthermore, Brummell et al. (1996) observe that while the components of the rotation vector tend to increase the isotropy in a wide range (from medium to small) of scales (compared to the non-rotating case, where the isotropy affects only the smallest scales Cattaneo et al. 1991), the strong rotation also introduces a preferred direction. Thus, the coherent structures of the turbulent flows have a tendency to align with the rotation vector under the action of the Coriolis force. This effect depends on the amplitude of the rotation. At the pole, the structures will be vertical, while on the equator these structures tend to be orientated with the rotation and form an angle with the vertical. This geometrical effect has the consequence of decreasing the energy available per surface unit in the vertical direction, and therefore of decreasing their ability to penetrate below the boundary. This seems to indicate that the effect of rotation in decreasing the depth of convective penetration should be more significant on the equator than at the pole.

In summary, although the positive buoyancy flux in the convective layer is not significantly altered by rotation, systematic changes are observed in the penetration zone. Firstly, the width of the region of negative buoyancy flux is also considerably reduced at high rotation. Hence the thickness of the penetration zone, defined by the difference between the maximum depth of penetration and the mixed layer depth, is significantly reduced at high rotation. Secondly, without rotation, a few strong plumes extend throughout the mixed layer. At high rotation, there are more but weaker plumes.

We should also mention other effects related to the rotation through the presence of magnetic fields, and that could affect the generation and propagation of internal waves. Indeed, Schatzman (1993), following a phenomenological treatment, shows that a concentration of magnetic field in the penetrative layer could filter the internal waves, the filter being more efficient as the rotation velocity increases. Recently, Barnes et al. (1998) have also studied how the magnetic field in a shear layer could alter the propagation of gravity waves.

We observe, then, that there is a great number of complex effects of rotation on the diffusion processes linked to the internal wave propagation. Even if a quantitative treatment of that problem is not tackled at the moment, all the effects abovementioned show the same tendency, which is to decrease the transport processes as the rotation increases.

In particular, we have seen that stellar rotation can modify the source function of internal waves, in terms of both its features and its location, and hence in the diffusion coefficient characteristics. Here we shall use a phenomenological approach to these effects on the source function in order to analyse how the rotation could produce a spread of lithium abundance in the framework of the proposed diffusion process.

We consider three different sources of scattering in lithium depletion:

- First, the initial dispersion. We cannot reproduce the lithium spread during the PMS since we do not have models earlier than 10^8 yr, but we can speculate and consider that a different efficiency of the overshooting due to the rotation during the PMS should provide significant dispersion of the lithium abundance when arriving on the main sequence. We will simulate this initial dispersion, using the observational data in the Pleiades, where the lithium dispersion seems "correlated" to the rotational dispersion. The transport process proposed must be able to reduce that dispersion as the ages of clusters increase. In the same way, it must be compatible with the rapid evolution of rotation from the age of the Pleiades to that of the Hyades (Stauffer 1991).
- Second, the two effects of rotation on the penetrative convection:
  1. Decrease in the depth of the penetration layer.
  2. Diminution of kinetic energy of plumes in the convective zone.

Despite its ubiquity, penetrative convection, and its role in the inherent organization on large scales, is to date elusive with regard to a comprehensive and quantitative understanding of the physical processes involved. In all attempts to estimate the extent of solar convective overshooting many effects, such as magnetism, ionization and rotation, have been neglected. Recent results show, however, the constraining effect of rotation on convective penetration. Unfortunately, at the moment there does not exist any model, either parameterizations which allow a function to be built relating the rotational velocity and the depth of the penetrative layer, or relating stellar rotation and kinetic energy in the plumes. Neither do we know the description of turbulent motions in the braking layer itself. Therefore, we shall be satisfied here if we can do some parametric analysis. In order to study the influence of the depth of the penetrative layer, we calculate the evolution of lithium abundance using stellar models computed with two different values of the parameter of convective penetration. On the other hand, to take into account the effect of decreasing the mean square velocity of motions at the boundary of the turbulent region, we shall modify the value of $V_{\rm M}$ in the diffusion coefficient expression (Eq. 29). The diffusion coefficient, in addition to stellar structure, depends on the characteristics of turbulence describing the motion at the boundary of the convective zone; that is, on the mean square velocity of turbulent flow, and on the characteristic size of turbulent elements. Both parameters have been estimated from the Rieutord & Zahn (1995) model of convection by plumes, and from laboratory measurements of parameters describing the turbulence in the interior of the plumes (List 1982). Now, according to the numerical simulations by Julien et al. (1996a,b), the sizes of plumes and their velocities decrease as the rotation increases. Since we do not have any relation allowing us to estimate how much $V_{\rm M}$ decreases as a function of stellar rotation, we use a simple parameterization; we consider two cases: a diminution in $V_{\rm M}$ by 10% that implies a decrease of 20% in the diffusion coefficient, and a diminution of 25% in $V_{\rm M}$ that implies a decrease of 50% in the diffusion coefficient.

In our models we always applied the same parameterization of the diffusion coefficient as a function of time. It would be better, however, to consider that the stars in the upper curve of lithium abundance (in principle rapid rotators) have smaller penetration and smaller velocity of turbulent flow. Nevertheless, as the star is braked by the stellar wind, the effect of rotation in reducing the overshooting is also reduced, and we should apply a more efficient diffusion coefficient. As the rotation evolution is very rapid, this less efficient diffusion coefficient should work for a short time. This involves a tendency to decrease the scattering with time, as is observed. In every case, we have applied the same diffusion coefficient for both curves. We realize that it would be more coherent to apply a less efficient diffusion coefficient to the upper curve at least during the period of rapid rotation. However, given the approximate character of these computations, we think that it would increase confusion to no advantage. In Fig. 4 we can also see the evolution of the original dispersion of lithium abundance in the Pleiades as a function of time. On the other hand, we observe that the effect of changing the overshooting is more important for low masses. In contrast, the effect of changing the mean square velocity of the turbulent flow has an effect over the entire mass range, but a diminution in $V_{\rm M}$ by 10% or 25% does not have very significant consequences. Nevertheless, we must bear in mind that we do not know anything concerning the diminution of the kinetic energy in the plumes due to the rotation, and the fact that if only 10% of the velocity of the plume remains, then the diffusion coefficient decreases by a factor 500! We do not experiment further with that parameter for the further reason that the decrease in the surface of the plume and the number of plumes should be taken into account, and for the moment we cannot apply any restriction.

We do not try, of course, to reproduce the dispersion of lithium abundances quantitatively, but we claim that convection, internal waves and stellar rotation are very complex physical processes, that interact among themselves, and that the level of knowledge and of modelling of these processes are not precise enough to reject the internal waves as the mechanism responsible for chemical mixing in low-mass stars. This transport process is not incompatible, within the present knowledge, with the presence of lithium dispersion at each mass and age, or with the diminution in dispersion as function of the age of the cluster. On the contrary, angular momentum loss (AML) models, which link lithium depletion to angular momentum losses, would predict, for a cluster like the Pleiades, which evolves from 10^8yr to 8.10^8 yr (the age of the Hyades), a lithium dispersion much larger than what is observed in the Hyades (Schatzman 1994; Montalbán 1995).

The lithium abundance evolution in binaries could also be explained. If a star rotates rapidly during an important part of its life, this means that, for a long period the diffusion process due to internal waves is much less efficient than for a star that has reduced its rotational velocity because of magnetic braking. So, the close binaries proposed as evidence for the validity of AML models, could also be explained within the framework of our model. One star that, at the age of the Hyades, has not been braked, has experienced a weak diffusion process, while another that began rotating quickly and was braked quickly, suffered a weak diffusion process only for a short time.

4.4. Beryllium abundance

Beryllium is also a light element that burns at $3.5\,10^6$ K, slightly deeper than the lithium burning level. Therefore, the complementary information that the Be abundance can provide is of great importance in discriminating between different mixing processes proposed to explain stellar lithium abundances. Unfortunately, observational data for beryllium are much scarcer than for lithium because the wavelengths of its lines makes good measurement difficult.

There are only few clusters or field stars having both Li and Be measurements in G- and K-type stars. García López et al. (1995) provided Be abundances in a sample of late-type stars with well known stellar parameter, five G- and K-type stars belonging to the Hyades open cluster and four K-type stars that are probably members of Ursa Major Group. Reliable abundances were observed for three Hyades stars with temperature in the range 5700–5200 K, and only upper limits in stars cooler than 5200 K. On the other hand, Stephens et al. (1997) present an extensive search for Be in lithium-deficient field stars. For near-solar metallicities ([Fe/H] ≥ -0.5), their sample has effective temperatures in the range 6800–5500 K. Warm stars ($T_{\rm eff} \geq 6100$ K) which populate the effective temperature regime typically associated with the Li abundance gap also exhibit significant Be deficiency. There is a wide range of Be abundance values, with a minimum near 6500 K. They interpret this as the Be analogue to the Boesgaard lithium gap. But, as for lithium in field stars, the correlation between Be abundances and effective temperature is washed out by age, chemical or evolutionary differences in this sample of stars. However, for cool stars ($T_{\rm eff} < 6100$ K), observational results present very different behaviour between the Li and Be abundances: Li-deficient stars do not appear to be significantly Be-poor. Thus, in Hyades stars, between $T_{\rm eff}$ = 5600 K and $T_{\rm eff}$ = 5200 K Li has decreased by 1.64 dex, and Be by only 0.2 dex. For the field-star sample, despite the difference in such stellar parameters as age and metallicity, observational data also reveal an almost constant value of Be abundance, and the measured abundances in cool solar ([Fe/H] $\geq$ –0.5) stars are at most depleted by a factor of ≈ 4 with respect to the meteoritic level. Cool stars belonging to open clusters or in field stars, then, show, as a general tendency, Be to be hardly depleted, even for masses for which a large lithium destruction is observed. Be abundance seems to not depend significantly on time and stellar mass.

This indicates that the efficiency of the transport process must decrease very quickly as the depth increases. In this way, the mechanism is able to transport lithium to the burning level, but not much deeper. This is the case for the internal wave diffusion process (Fig. 2), which decreases very quickly below the convective zone boundary.

In Fig. 4d we represent two pairs of curves corresponding to Be abundances at $1.\,10^8$ and $4.5\,10^9$ yr, predicted by the

diffusion coefficient linked to internal waves (Eq. 29). We also plot the observational data for the Hyades and Ursa Major Group (García López et al. 1995) and the field-star sample with solar metallicity (Stephens et al. 1997). We have done computations for two values of the initial Be abundance. Since, as Stephen et al. (1997) noticed, it is not clear if Be_0 must be taken at the meteoritic value (1.42, Anders & Grevesse 1989), or the value given by Boesgaard (1976), who found Be_0=1.11 as the average in F and G dwarfs. In these curves no PMS burning of beryllium has been taken into account. From the PMS models by D'Antona & Mazzitelli (1994) and Forestini (1994) it seems that Be is not significantly depleted during this phase. Estimates for a star of 0.8 $M_\odot$ give the result that only 1% of its beryllium has been destroyed during the PMS.

Be abundances predicted by our diffusion coefficient are compatible with the observational data in the effective temperature range considered. The dispersion and the large error-bars associated with these data do not allow us for the moment to give important complementary constraints for our diffusion model. It would be very useful to have Be abundances of late-type stars in open clusters in order to avoid the scatter due to difference in age or chemical composition, especially for effective temperatures lower than 5200 K.

On the other hand, it is necessary to solve the problem pointed out by Balachandran & Bell (1997) concerning the large error in Be abundance determinations due to the uncertain continuous opacity in the ultraviolet, where the Be II lines are found. According to this paper, Be abundances would be usually underestimated, and the Sun would not have depleted its initial Be content.

5. Summary and conclusions

We have presented here a model which relates the lithium depletion problem with the turbulent motions in the convective envelopes of stars. It concerns a diffusive process produced by the non-adiabatic propagation of internal waves excited in the stable region by turbulent elements in the convective zone. In order to characterize the source of these waves, their amplitude and frequency spectrum we used a model of the convective transport of heat different from the MLT model. This model is based on numerical simulations, geophysical flows and laboratory experiments. So the transport of energy is performed by large vertical structures (plumes) crossing the convective zone (modelled by Rieutord & Zahn 1995); these plumes are braked by the stratification and are able to penetrate in the radiative region until they have null velocity (overshooting following Zahn 1991). Furthermore, the numerical simulations by Julien et al. (1997a) predict a decrease in convective penetration depth and in the energy of the plumes in the penetration layer (where internal waves are excited) as the rotation increases.

This model of the generation of internal waves provided the following results:

– The expression for the diffusion coefficient presents different dependences on the characteristic scales of velocity and wavenumber of turbulence, and on the depths below the bottom of the convective zone, but it is not significantly different from that obtained in Paper I and Paper II. However, due to the asymmetric nature of the vertical motions (with more energetic and concentrated downward structures) in the model of the convective transport, the kinetic energy available for exciting the internal waves is greater than in the MLT case, and hence it is not necessary to introduce any arbitrary parameter to increase the amplitude of the internal waves generated, as was the case in apers using MLT (García López & Spruit 1991; Schatzman 1991; Montalbán 1994).
– We have used that diffusion coefficient to calculate the lithium abundance in stars with masses between 0.7 and 1.2 $M_\odot$ and ages between 8.10^8 and 5.10^9 yr. These predictions are successfully compared with the lithium abundances observed in several open clusters. The comparison shows that the transport process induced by internal waves is able to reproduce the dependence of lithium abundance on spectral type and on age.
– This transport process is also consistent with the presence of the spread of lithium abundance and its apparent relationship with stellar rotation. Numerical simulations show that the energy of the downward plumes in the penetrative region (where the internal waves are excited) and the depth of this region decrease as the stellar rotation increases. Hence, given the dependence of the diffusion coefficient on the kinetic energy of the flow in the plumes and on the depth below the mixed region, the transport process induced by internal waves is much less efficient in a fast rotator than in a slow rotator. Therefore, a star spending a large fraction of its life as a rapid rotator presents a larger lithium abundance than a similar star with the same age, mass and chemical composition, but different rotational evolution. The tendency of lithium abundance in close binaries is equally explained within this framework. So a different history of angular momentum loss produces stars that have suffered a mixing process of internal waves with different efficiency; hence it would be possible to explain the rotation–lithium abundance "correlation" without directly connecting the angular momentum loss process to the chemical mixing mechanism. Finally, the observed tendency of the scatter to decrease with age is also qualitatively reproduced.
– The prediction of Be abundance and the comparison with observations should be useful for testing if the dependence on the depth below the mixed region agrees with the behaviour expected. Be abundances predicted for stars with masses between 0.7 and 1.2 $M_\odot$ are within the error-bars (which are quite large). However, there are limited observational data in the effective temperature range covered by our models, most of the observational data corresponding to the lithium-gap domain, and for fields stars which present a great dispersion in age and metallicity. More observations for $T_{\rm eff} < 6000$ K and more accurate data are needed in order to be able to use the Be abundance as a criterion for discriminating between the various physical processes pro-

posed. Furthermore, it is necessary to solve the problem pointed out by Balachandran & Bell (1997), concerning the uncertainty in the determination of Be abundance from observed spectra.

We therefore conclude that a more physically consistent treatment of the problem of the generation of internal waves by the convective zone could provide a transport process able to reproduce not only the dependence on the effective temperature and age of the light element abundance, but also the scatter in the observations, and its connection to stellar rotation. In the present state of the art of stellar rotation and stellar convection, the results of this work show that the transport process induced by internal waves cannot be rejected; on the contrary, it provides a coherent explanation of the different observational aspects of the lithium problem in the range of effective temperatures lower than $\simeq 6200$ K; that is, below the so called "lithium dip" (Boesgaard & Tripico 1986). However, García López & Spruit (1991) studied this domain, also considering a transport process linked to the propagation of internal waves. As mentioned above, it was necessary to increase *ad hoc* the convective velocity provided by the MLT in order to be able to reproduce the observational data. We could then presume that an adequate treatment of convection in shallow convective layers characteristic of F-type stars could provide more realistic velocities and hence reproduce also the lithium abundance in the narrow domain of lithium gap.

A great effort is still necessary on the observational and theoretical fronts in order to add new constraints to the characteristic of the transport mechanisms working inside stars. In the observational domain, a large and significant sample of Be abundances would be useful; in the theoretical domain, a deep knowledge of physical processes such as rotation and convection, and their interaction could provide information about the real mixing process linked to the differential rotation, and quantitative relationships between stellar rotation, the energy of plumes, and the depth of the overshooting.

References

Anders E., Grevesse N., 1989, Geochim. Cosmochim. Acta 53, 197
Asaeda T., Imberger J., 1993, J. Fluid Mech. 249, 35
Balachandran S., Lambert D.L. Stauffer J.R., 1988, ApJ 333, 267
Balachandran S. 1995, ApJ 446, 203
Balachandran S., Bell R.A., 1997, A&AS 191, 7408
Baglin A., Morel P., Schatzman E., 1985, A&A 149, 309
Barnes G., MacFregor K.B., Charbonneau P., 1998, ApJ 498, L169
Berthomieu G., Morel P., Provost J., Zahn J.-P., 1993, In: Weiss W.W., Baglin A. (eds.) Inside the Stars. IAU Colloquium 137, ASP Conference Series Vol. 40, p. 60
Boesgaard A.M., 1976, ApJ 210, 446
Boesgaard A.M., Tripico M.J., 1986, ApJ 302, L49
Boesgaard A.M., Friel E.D., 1990, ApJ 351, 467
Boesgaard A.M., Budge, K.G., Ramsay M.E., 1988, ApJ 327, 389
Bretherton F.P., 1969, J. Fluid Mech. 36, 785
Brummell N.H., Hurlburt N.E., Toomre J., 1996, ApJ 473, 494
Carruthers D.J., Hunt J.C.R., 1986, J. Fluid Mech. 165, 475
Cattaneo R., Brummell N.H., Toomre J., Malagoli A., Hurlburt N.E., 1991, ApJ 370, 282
Cayrel R., Cayrel de Strobel G., Campbell B., Däppen W., 1984, ApJ 238, 205
Chaboyer B., Demarque P., Pinsonneault M.H., 1995, ApJ 441, 865
Chaboyer B., Zahn J.-P., 1992, A&A 253, 173
Chandrasekhar S., 1943, Rev. Mod. Phys. 15, 1
D'Antona F., Mazzitelli I., 1994, ApJS 90, 467
Duncan D.K., 1981, ApJ 248, 651
Duncan D.K., Jones B.F., 1983, ApJ 271, 663
Eff-Darwich A., Korzennik S.G., 1998, In: Structure and Dynamics of the Interior of the Sun and Sun-like stars. Proceeding of the SOHO 6/GONG 98 Workshop, ESA SP-418, p. 685
Forestini M., 1994, A&A 285, 473
García López R.J., Spruit H., 1991, ApJ 337, 268
García López R.J., Rebolo R., Martí E.L., 1994, A&A 282, 518
Grimshaw R., 1972, J. Fluid Mech. 54, 193
Hoobs L.M., Pilachowski C.A., 1986, ApJ 311, L37
Huebner W.F., Merts A.L., Magee N.H., Argo M.F., 1977, In: Los Alamos Sci. Lab. Rep. n^o-LA-6760-M
Hurlburt N.E., Toomre J., Massaguer J.M., 1986, ApJ 311, 563
Hurlburt N.E., Toomre J., Massaguer J.M., Zahn J.-P., 1994, ApJ 421, 245
James D.J., Jeffries R.D., 1997, MNRAS 291, 252
Janes K.A., Tilley C., Lyngå G., 1988, AJ 95, 771
Jeffries R.D., 1997, MNRAS 292, 177
Jones B.F., Fischer D., Shetrone M., Soderblom D.R., 1997, AJ 114, 352 (M 34)
Julien K., Legg S., McWilliambs J., Werne J., 1996a, Dyn. Atmospheres and Oceans 24, 237
Julien K., Legg S., McWilliambs J., Werne J., 1996b, J. Fluid Mech. 322, 243
Julien K., Werne J., Legg S., McWilliambs J., 1997a, In: Pijpers E.P., Chistensen-Dalsgaard J., Rosental C.S. (eds.) SCORc'96: Solar Convection and Oscillations and their Relationship. Proceedings of a workshop in Aarhus, Denmark, May 1996, Astrophysical and Space Science Library Vol. 225, p. 227
Julien K., Werne J., Legg S., McWilliambs J., 1997b, In: Pijpers E.P., Chistensen-Dalsgaard J., Rosental C.S. (eds.) SCORc'96: Solar Convection and Oscillations and their Relationship. Proceedings of a workshop in Aarhus, Denmark, May 1996, Astrophysical and Space Science Library Vol. 225, p. 331
Kurucz R.L., 1991, In: Crivellari L., Hubeny I., Hummer D.G. (eds.) Stellar Atmospheres beyond the Classical Model. NATO ASI Series, Kluwer, Dordrecht, p. 441
List E., 1982, J. Ann. Rev. Fluid Mech. 14, 189
Martín E.L., Claret A., 1996, A&A 306, 408
Martín E.L., Magazzù A., Rebolo R., 1994, A&A 282, 503
Massaguer J.M., 1990, In: Goupil M.-J., Zahn J.-P. (eds.) Rotation and Mixing in Stellar Interiors. Lecture Notes in Physics 366, p. 129
McIntyre M.E., 1973, J. Fluid Mech. 60, 801
Michaud G., Charbonneau P., 1991, Space Sci. Rev. 57, 1
Montalbán J., 1994, ApJ 281, 421 (Paper I)
Montalbán J., 1995, Ph.D. Thesis, Paris-7
Montalbán J., Schatzman E., 1996, A&A 305, 513 (Paper II)
Morel P., 1992, Private Communication
Morton B.R., Taylor G.I., Turner J.S., 1956, Proc. R. Soc. Lond. A 234, 1
Pasquini L., Randich S., Pallavicini R., 1997, A&A 325, 535
Pasquini L., Liu Q., Pallavicini R., 1994, A&A 287, 91
Pinsonneault M.H., Kawaler S.D., Sofia S., Demarque P., 1989, ApJ 338, 424
Pinsonneault M.H., Kawaler S.D., Demarque P., 1990, ApJS 74, 501

Press W.H., 1981, ApJ 245, 286
Rayleigh Lord, 1899, In: Scientific Papers Vl.IV, Cambridge University Press, p. 370
Rieutord M., Zahn J.P., 1995, A&A 296, 127 (RZ95)
Rogers F.J., Iglesias C.A., 1992, ApJS 79, 507
Schatzman E., 1991, In: Cox A.N., Livingston W.C., Matthews M.S. (eds.) Solar Atmosphere and Interior. Space Sci. Ser., University of Arizona Press, p. 192
Schatzman E., 1993, A&A 271,L29
Schatzman E., 1994, In: Processus de transport, Aussois 1994, Published by Observatoire de Paris
Schatzman E., 1996, J. Fluid Mech. 322, 355
Schatzman E., Montalbán J., 1995, in Roxburgh I.W., Masnou J.-L. (eds.) Physical Processes in Astrophysics. Lecture Notes in Physics 458, p. 171
Schmitt J.H.H.M., Rosner R., Bohn H.U., 1984, ApJ 282, 316
Soderblom D.R., Oey M.S., Johnson D.R.H., Stone R.P.S., 1990, AJ 99, 595
Soderblom D.R., Pilachowski C.A., Fedele S.B., Jones B.J., 1993a, AJ 105, 2299
Soderblom D.R., Jones B.J., Balachandran S., et al., 1993b, AJ 106, 1059 (Pleiades)
Soderblom D.R., Fedele S.B., Jones B.J., Stauffer J.R., Prosser C.F., 1993c, AJ 106, 1080 (praesepe)
Soderblom D.R, Jones B.J., Stauffer J.R., Chaboyer B., 1995, AJ 110, 729 (Hyades enanas K, litio)
Spruit, H.C., Nordlund Å., Title A.M., 1990, Ann. Rev. Asrop. Ap 28, 263
Stauffer J.R., 1991, In: Catalano S., Stauffer J.R. (eds.) Angular Momentum Evolution of Young Stars. Kluwer Academic Publisher, p. 117
Stein R.F., Nordlund A., 1989, ApJ 342, L95
Stephens A., Boesgaard A.M., King J.R., Deliyannis C.P., 1997, ApJ 491, 339
Strobel A., 1991, A&A 247, 35
Thorburn J.A., Hobbs L.H., Deliyannis C.P., Pinsonneault M.H., 1993, ApJ 415, 150
Townsend A.A., 1966, J. Fluid Mech. 24, 307
Turner J.S., 1986, J. Fluid Mech. 173, 431
Unno W., Osaki Y., Ando H., Shibahash H., 1989, Non-radial oscillations of stars. 2nd ed., University of Tokyo Press, Tokyo
Zahn J.-P., 1991, A&A 252, 179
Zahn J.-P., 1992, A&A 256, 115